

Dynamics and Control of Robotic Systems Worn by Humans

H. Kazerooni, S. L. Mahoney

Mechanical Engineering Department
University of Minnesota, Minneapolis, MN 55455

Abstract

This article describes the dynamics, control, and stability of extenders, robotic systems worn by humans for material handling tasks. Extenders are defined as robot manipulators which extend (i.e., increase) the strength of the human arm in load maneuvering tasks, while the human maintains control of the task. Part of the extender motion is caused by physical power from the human; the rest of the extender motion results from force signals measured at the physical interfaces between the human and the extender, and the load and the extender. Therefore, the human wearing the extender exchanges both power and information signals with the extender. The control technique described here lets the designer define an arbitrary relationship between the human force and the load force. A set of experiments on a two-dimensional non-direct-drive extender were done to verify the control theory.

Introduction

This article describes the dynamics and control of a human-integrated material handling system. This material handling equipment is a robotic system worn by humans to increase human mechanical ability, while the human's intellect serves as the central intelligent control system for manipulating the load. These robots are called extenders due to a feature which distinguishes them from autonomous robots: they extend human strength while in physical contact with a human. The human becomes a part of the extender, and "feels" a force that is related to the load carried by the extender.

Figure 1 shows an example of an extender. Some major applications for extenders include loading and unloading of missiles on aircraft; maneuvering of cargo in shipyards, foundries, and mines; or any application which requires precise and complex movement of heavy objects.

The goal of this research is to determine the ground rules for a control system which lets us arbitrarily specify a relationship between the human force and the load force. In a simple case, the force the human feels is equal to a scaled-down version of the load force: for example, for every 100 pounds of load, the human feels 5 pounds while the extender supports 95 pounds. In another example, if the object being manipulated is a

pneumatic jackhammer, we may want to both filter and decrease the jackhammer forces: then, the human feels only the low-frequency, scaled-down components of the forces that the extender experiences. Note that force reflection occurs naturally in the extender, so the human arm feels a scaled-down version of the actual forces on the extender without a separate set of actuators. See reference 5 for a brief history on human amplifiers [1-4 and 11-15].

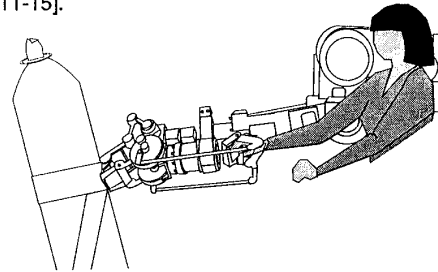


Figure 1: The extender supports an arbitrary portion of the force associated with maneuvering an object, while a human supports the rest of the load.

Dynamic Modeling

This section models the dynamic behavior of the Figure 1 elements: the extender, the environment (i.e., the object being manipulated), and the human.

Extender Model

The extender is assumed to have either a closed-loop position controller or a closed-loop velocity controller¹. Throughout this article, this controller is called a *primary stabilizing controller*. The resulting closed-loop system is called a *primary closed-loop system*. The following motivated our choosing a closed-loop primary stabilizing controller for the extender.

1. A closed-loop velocity or positioning control system eliminates the effects of frictional forces in the joints and in the transmission mechanism, and creates a more definite dynamic behavior in the robot. Minimizing the effects of uncertainty in the system is

¹In the experiments discussed later, a position control system was used.

a usual design specification for position controllers. (See references 6 and 17 for two linear design methods).

2. A closed-loop velocity or position control system creates linear dynamic behavior in the extender. Here we assume that, for non-linear robot dynamics, a nonlinear stabilizing controller has been designed to yield a nearly linear closed-loop position (or a closed-loop velocity) system for robotic systems [16]. This lets us assume that the extender closed-loop dynamics can be approximated by transfer function matrices. See reference 5 for a nonlinear analysis of the dynamics and control of extenders.
3. Choosing a closed-loop positioning system for the extender lets the designers deal with the robustness of the extender without being concerned with the dynamics of the human or the environment. These dynamics change with each operator and environment.
4. Human safety dictates that the extender remain stable when not worn by a human. A closed-loop velocity or position control system keeps the extender stationary when not being worn.

In equation 1 below, the vector, p , represents the position of the extender in a Cartesian coordinate frame². The extender position, p , is a function of u , the electronic input command to the primary closed-loop system; f_h , the force from the human; and f_e , the force from the environment. As shown in Figure 2, three transfer function matrices G , S_h , and S_e represent the effects of u , f_h , and f_e , respectively. G represents the closed-loop transfer function of the extender primary closed-loop positioning system. Regardless of whether a position controller or velocity controller is selected as the primary stabilizing controller, the output of G is considered to be the extender position. The internal feedback loops associated with the primary stabilizing controller are not explicitly shown in the block diagram. S_h is the sensitivity of the extender closed-loop positioning system to f_h , the forces imposed by the human operator. Similarly, S_e is the sensitivity of the extender closed-loop positioning system to f_e , the forces imposed by the environment; S_e shows how f_e disturbs the extender position. With the above variables, the extender position can be expressed as:

$$p = G u + S_h f_h + S_e f_e \quad (1)$$

Note that G , S_h , and S_e depend on the nature of the extender primary stabilizing controller. In particular, they vary depending on whether a position or velocity control system is chosen, and on the particular compensator chosen for the closed-loop positioning system. If a compensator with several integrators is chosen to insure small steady state errors, then S_h and S_e will be small in comparison to G . If the extender

actuators are non-backdrivable, then S_h and S_e will be small regardless of how carefully the robot's positioning compensator is chosen.

Human Arm Model

Human arm maneuvers fall into two categories: *unconstrained* and *constrained*. In unconstrained maneuvers, the human arm is not in contact with any object, while, in constrained maneuvers, the human arm is in constant with an object continuously. Since the human arm wearing the extender is always in contact with the extender, our primary focus is on constrained maneuvers of the human arm.

The force imposed by the human arm on the extender results from two inputs. The first input, m_h , is the force imposed by the human muscles, and the second input is the motion (position and/or velocity) of the extender. It is assumed that the specified form of m_h is not known other than that it is the result of human thought deciding to impose a force onto the extender. The dynamic behavior in the generation of m_h by the human central nervous system is of little importance in this analysis since it does not affect the system performance and stability. One can think of the extender motion as a position disturbance occurring on the force-controlled human arm. If the extender is stationary, the force imposed on the extender is a function only of muscle forces. However, if the extender moves, the force imposed on the extender is a function not only of the muscle forces but also of the motion of the extender (i.e., velocity and/or position). In other words, the human contact force with the extender will be disturbed and will be different from m_h , if the extender is in motion. H is defined in equation 2 to map the extender position, p , onto the contact force, f_h .

$$f_h = m_h - H p \quad (2)$$

H is the human arm impedance and is determined primarily by the physical properties of the human arm. The section on experimental results discusses an example of H and how it is measured.

Environment Model

The extender is used to manipulate heavy objects or to impose large forces on objects. The force created between the robot and environment, f_e , is a function of the environment dynamics and the extender motion. Defining E as a transfer function matrix representing the environmental dynamics and n_e as the equivalent of all the external forces imposed on the environment, equation 3 provides a general expression for the force on the extender, f_e , as a function of p .

$$f_e = n_e - E p \quad (3)$$

At the summing junction in figure 2, the sign on E is negative because if the extender moves abruptly along the positive direction of an axis the environment, E , impedes the extender's motion. The extender feels a force in the negative direction and the environment feels an equal force in the positive direction. If the extender is

² All matrices and vectors are $n \times n$ and $n \times 1$, unless otherwise stated. n is the number of degrees of freedom of the extender.

used to manipulate a mass m along the x direction $E = m s^2$ and $f_e = -m s^2 x$ if $n_e = 0$.

Note that f_e is measured by a force sensor near the robot's endpoint. Everything forward of this sensor is considered to be part of the environment.

The Control Architecture

The controller consists of two compensators K_h and K_e . The compensators map the extender's contact forces f_h and f_e to u , the input to the extender's primary closed-loop system.

$$u = K_h f_h + K_e f_e \quad (4)$$

Figure 2 depicts how the extender, environment, and human interact dynamically. Examining figure 2 reveals that K_h and K_e provide additional paths for f_h and f_e to map to p . The physical contact between the human and the extender produces some extender motion as f_h acts through S_h . In general, S_h is much smaller than desired: thus, the human operator alone does not have sufficient strength to move the extender and load as desired. An additional route for f_h to map to p can be added if K_h is chosen to be non-zero; K_h can be thought of as the component that shapes the overall mapping of the force f_h to the position p . This leads to an effective sensitivity of $(S_h + G K_h)$ [7].

G and S_h are fixed by the mechanical design of the extender and by the chosen primary stabilizing controller. The designer has some freedom (limited by stability considerations) to adjust the effective sensitivity $(S_h + G K_h)$ along the path from f_h to p . Assuming for a moment that E and n_e are zero, $(S_h + G K_h)$ affects how the extender "feels" to the human operator. For instance, if K_h is chosen so $(S_h + G K_h)$ is approximately a constant, the extender reacts like a spring in response to f_h . Similarly, if $(S_h + G K_h)$ is approximately a single or double integrator, the extender acts like a damper or mass, respectively.

The notion of interaction via the transfer of *power* and *information signals* can be clarified here. The actual force of f_h affects the extender motion via S_h thus transferring power to the extender. The measure of f_h affects the extender motion through $G K_h$ thus transferring information signals to the extender.

As the block diagram in figure 2 suggests, there is a duality between the human and environment. Hence, K_e serves to adjust the admittance from f_e to P , just as K_h adjusts the admittance from f_h to P . The resulting sensitivity to f_e is $(S_e + G K_e)$. If no operator wears the extender (i.e., H and m_h are zero), K_e could be used to adjust how the extender would react to f_e (i.e., compliant [8], damped, etc.). The concept of transfer of power and information signals is also valid for the load and extender. S_e represents the path by which the actual force of f_e affects the extender (power transfer), while

$G K_e$ represents the path by which the measure of f_e affects the extender motion (information signal transfer).

Performance

Suppose the extender is employed to

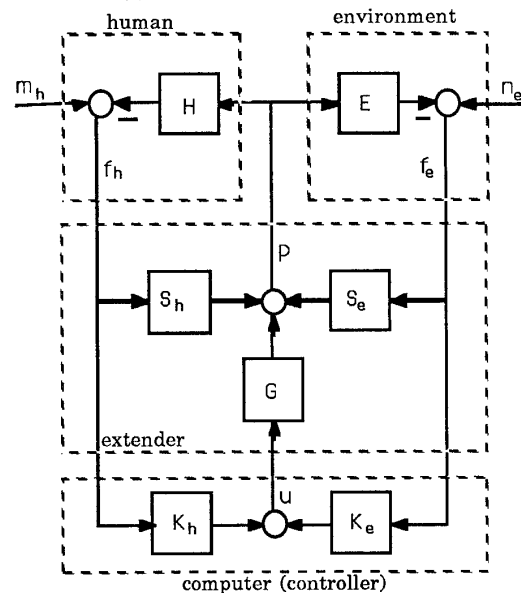


Figure 2: S_h and S_e represent the power transfer paths to the extender, while $G K_h$ and $G K_e$ represent the information signal transfer paths to the extender.

manipulate an object through a completely arbitrary trajectory. It is reasonable to ask for an extender dynamic behavior where the human feels a scaled-down version of the load forces on the extender: that is, the human has a natural sensation of the forces required to maneuver the load (i.e., the acceleration, gravitational, coriolis and centrifugal forces associated with an arbitrary maneuver). This example calls for masking the dynamic behavior of the extender, human, and load via the design of K_e and K_h to create a desired relationship between f_h and f_e . Therefore, the objective is to choose K_e and K_h so:

$$f_e = -\alpha f_h \quad (5)$$

In general, α is a transfer function matrix and is referred to as the performance matrix. In the above example, α should be chosen as a diagonal transfer function matrix with all members larger than unity representing force amplification. This would effectively increase human strength by a factor of α . In another example, suppose an extender is used to hold a jackhammer. The objective is to decrease and filter the force transferred to the human arm so the human feels only the low-frequency force components. This requires that α^{-1} be a diagonal matrix with low-pass filter transfer functions as its members.

Note that the performance specification expressed by equation 5 does not assure the stability of the system in Figure 2 but does let designers express what they wish to have happen during a maneuver if instability does not occur. Inspection of Figure 2 results in equation 6 as a relationship between f_e and f_h .

$$f_e = -[I + E G K_e]^{-1} E G K_h f_h \quad (6)$$

Assuming that G does not have any right-half-plane zeros, K_h is chosen as:

$$K_h = [G^{-1} E^{-1} + K_e] \alpha \quad (7)$$

where α is the performance matrix specified by the designer. Limited by the stability condition discussed below, K_e is also the designer's option. Substituting for K_h from equation 7 into equation 6 results in equation 5. However, $G^{-1} E^{-1}$ may result in an unrealizable transfer function matrix for $[G^{-1} E^{-1} + K_e]$. It is recommended that K_h be chosen as:

$$K_h = [G^{-1} E^{-1} + K_e] \Delta \alpha \quad (8)$$

where Δ is a unity transfer function matrix at low frequencies with sufficient stable poles at higher frequencies to make K_h realizable. Δ represents the dynamics caused by implementing a realizable and reduced order K_h .

Closed-loop Stability

Instability may occur in the system when a large value is chosen for the compensator K_h . Suppose K_h has a large gain over a certain frequency range of operation. Then, if the human decides to move the object upward, the extender moves upward with such a large velocity that it jerks the human arm upward. This reverses the direction of the contact force, f_h (downward in Figure 1). Then the extender responds to this downward force with a large velocity which pulls the human arm downward. This periodic motion occurs in a very short amount of time and the motion of the extender becomes oscillatory and unbounded. K_h must be designed so its gain is large enough for the human to maneuver an object with high speed while stability is guaranteed. The above description is also true when K_e has a large gain over a frequency range of operation. Stability of the closed-loop system of Figure 2 depends on the location of the closed-loop poles. Inspection of Figure 2 reveals that equation 9 is the characteristic equation of the closed-loop system.

$$\det [I + G K_h H + G K_e E] = 0 \quad (9)$$

Substituting K_h from equation 8 into equation 9 results in equation 10 for the characteristic equation.

$$\det [I + G K_e E] \det [E^{-1}] \det [E + \Delta \alpha H] = 0 \quad (10)$$

The poles of the closed-loop system are the roots of three determinants. Since $\det [E^{-1}]$ represents the characteristics of a passive system, $\det [E^{-1}] = 0$ always results in stable poles. The first determinant, $\det [I + G K_e E]$, represents the characteristic equation

of the system of the environment-extender interaction when the human is not wearing the extender. The designers must choose K_e so the roots of $\det [I + G K_e E] = 0$ lie in the left half plane. One conservative condition that guarantees the roots of $\det [I + G K_e E] = 0$ are always in the left half plane is given by inequality 11:

$$\sigma_{\max} [K_e] < \frac{1}{\sigma_{\max} [GE]} \quad (11)$$

A large K_e results in a system that is compliant in response to the environmental forces. According to inequality 11, the larger E is, the smaller K_e must be. The upper bound on K_e is established by the maximum load the extender manipulates. In the limit when the environment is infinitely rigid, no K_e can be found to stabilize the system. Inequality 11 is a subclass of the general stability condition for the interaction of a robot with an environment (derived in references 7, 9, and 10).

Assume for a moment that $\Delta = I$. Then $[E + \alpha H]$ represents the total impedance that the extender encounters: an environment impedance and an equivalent *stronger human* impedance. Since both E and H represent passive dynamical systems, in the presence of $\Delta = I$, $[E + \alpha H]$ always results in stable roots, if α is chosen to be constant. In other words, once K_e is chosen to yield stable roots for $\det [I + G K_e E] = 0$ (or more conservatively to satisfy inequality 11), then the system is theoretically stable for all values of constant α if $\Delta = I$. However, when Δ is not unity, and/or α is an arbitrary transfer function, then the system stability depends on the roots of $\det [E + \Delta \alpha H] = 0$. In general, Δ is a stable transfer function with unity gain for a bounded frequency range and poles (perhaps with little damping) located at frequencies larger than the bandwidth of G. Therefore, we recommend that α be chosen as a low-pass filter to attenuate the effects of under-damped poles of Δ . This results in force amplification by a factor of α only within a limited bandwidth. If a wider bandwidth is required for force amplification, a correspondingly wider bandwidth is required for Δ . This requires a more complicated implementation of K_h (i.e., more poles and zeros), since Δ represents the dynamics ignored in implementing K_h . For a given Δ , one must compromise either on the size or the bandwidth of α . In other words, the designers can achieve a large force amplification only for a limited bandwidth or small force amplification for a wide bandwidth. (See "You Can't Always Get What You Want" by Mick Jagger.)

Experiment

Figure 3 shows the experimental setup: an xY table is employed as an experimental extender to verify the extender performance. The operator's hand grasps a handle mounted on a force sensor. A two-dimensional planar coordinate frame, xY , is chosen along the motor

axes directions as shown in Figure 3. The experimental system has two degrees of freedom; therefore, $n=2$, and all matrices and vectors are 2×2 and 2×1 for this experiment. A piezoelectric force sensor between the handle and the table measures the human's force, f_h , along the x and y directions. A mass is suspended below the platform from a force sensor. This force sensor measures the force imposed on the extender by the environment, f_e , along x and y directions. In addition, other sensing devices include a tachometer and an encoder (with a corresponding counter) to measure the speed and position of the table. A microcomputer is used for data acquisition and control.

In the experiments, we first determine the dynamic behavior of each element of the system: extender, human, and the load being maneuvered. The primary stabilizing controller for the xy table is designed to yield the widest bandwidth for the closed-loop transfer function matrix, G , and yet guarantee the stability of the closed-loop positioning system in the presence of bounded unmodeled dynamics in the table. (The development of the position controllers for the table has been omitted for brevity.) Due to the uncoupling of the xy table dynamics, G is a diagonal transfer function matrix in an xy coordinate frame. Due to the low pitch angle of the lead-screw mechanism, the xy table is not backdrivable: the table does not move under the forces exerted on the handle by the human, and S_e and S_h are virtually zero. If we assume $u = [u_x \ u_y]^T$ and $p = [x \ y]^T$, then G , introduced by equation 12, is a 2×2 transfer function matrix :

$$G = \begin{pmatrix} G_x & 0 \\ 0 & G_y \end{pmatrix} \quad \text{cm/cm} \quad (12)$$

The analytical values for G which represent the closed-loop positioning system for the table along the x and y directions are given by equations 13 and 14.

$$G_x = \frac{1}{\left(\frac{s^2}{31^2} + \frac{s}{25} + 1\right) \left(\frac{s^2}{265^2} + \frac{s}{294} + 1\right)} \quad (13)$$

$$G_y = \frac{1}{\left(\frac{s^2}{12.2^2} + \frac{s}{13.4} + 1\right) \left(\frac{s^2}{275^2} + \frac{s}{196} + 1\right)} \quad (14)$$

The above transfer functions are verified experimentally via a frequency response method.

If the human arm behaves linearly in the neighborhood of the horizontal position, H is the human arm impedance. For the experiment, the author gripped the handle, and the extender was commanded to oscillate along the x and y directions via sinusoidal functions. At each oscillation frequency, the operator tried to move his hand to follow the extender so that zero contact force was maintained between his hand and the extender. Since the human arm cannot keep up with the high-frequency motion of the extender when trying to maintain zero contact forces, large contact forces and consequently, a large H are expected at high frequencies. Since this force is equal to the product of

the extender acceleration and human arm inertia (Newton's Second Law), at least a second-order transfer function is expected for H at high frequencies. On the other hand, at low frequencies (in particular at DC), since the operator can follow the extender motion comfortably, he can always establish almost constant contact forces between his hand and the extender. This leads to the assumption of a constant transfer function for H at low frequencies where contact forces are small for all values of extender position. Based on several experiments, at various frequencies, the best estimates for the author's hand sensitivity along the x and y directions are presented by equations 15 and 16.

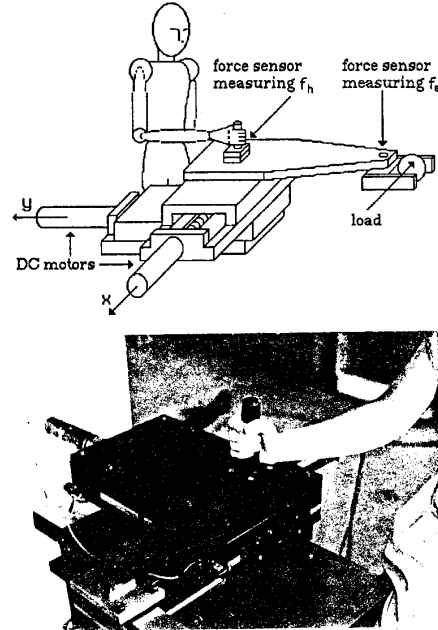


Figure 3: A schematic view of the xy table extender system

$$H_x = 0.1 \left(\frac{s^2}{2.5^2} + \frac{s}{2.19} + 1 \right) \text{ N/cm} \quad (15)$$

$$H_y = 0.125 \left(\frac{s^2}{2.75^2} + \frac{s}{1.83} + 1 \right) \text{ N/cm} \quad (16)$$

Figure 4 shows the experimental values and the fitted transfer functions (equations 15 and 16) for the human arm dynamic behavior.

The table is employed to move a mass (as shown in Figure 3). E is a diagonal matrix and, adopting notation similar to that of G in equation 12, its members are defined as:

$$E_x = 5 \text{ s}^2 \text{ N/cm (for all } \omega < 65 \text{ rad/sec)} \quad (17)$$

$$E_y = 5 \text{ s}^2 \text{ N/cm (for all } \omega < 65 \text{ rad/sec)} \quad (18)$$

The goal of the experiment is to decrease the force transferred to the human arm so the human feels scaled-down values of the force imposed by the load on the

table. Figure 5 shows the top view of the experiment where x^*y^* represents the coordinate frame in which the system performance is described.

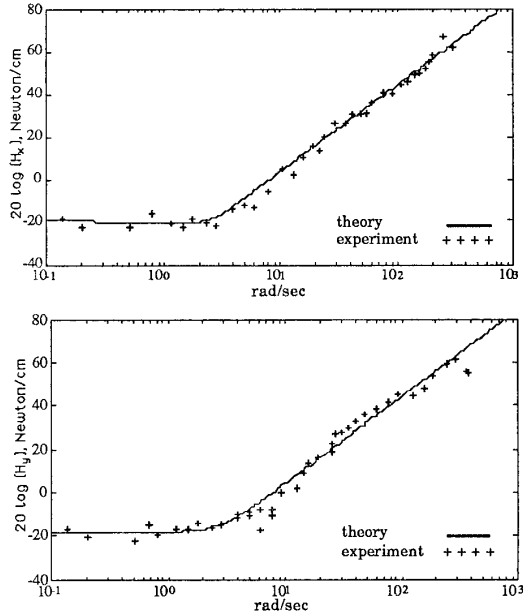


Figure 4: Human Arm Dynamics, H, Along the x and y Directions

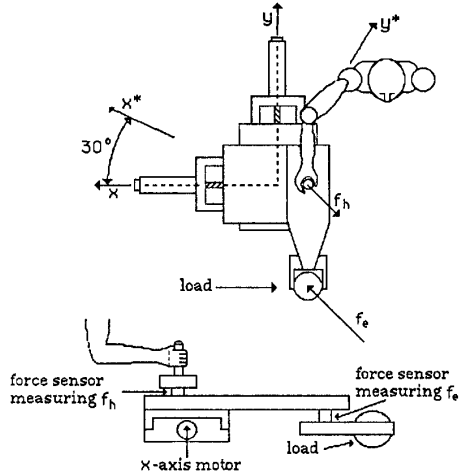


Figure 5: The x^*y^* coordinate frame, rotated 30° from the xy coordinate frame, is employed to define the force amplification along the x^* and y^* directions.

The design objective is to create a relation between the human forces and the environment force such that:

$$\begin{bmatrix} f_{ex}^* \\ f_{ey}^* \end{bmatrix} = -\alpha^* \begin{bmatrix} f_{hx}^* \\ f_{hy}^* \end{bmatrix} \quad (19)$$

where $[f_{ex}^* \ f_{ey}^*]^T$ and $[f_{hx}^* \ f_{hy}^*]^T$ represent the environment force and the human force in the x^*y^* coordinate frame. Matrix α^* is the performance matrix in the x^*y^* coordinate frame and is given by equation 20.

$$\alpha^* = \begin{bmatrix} 5 & 0 \\ 0 & 2 \end{bmatrix} \quad (20)$$

The above performance specification implies force amplifications of 5 times and 2 times along the x^* and y^* directions respectively. Translation of the above performance into the xy coordinate frame results in a non-diagonal performance matrix in the xy coordinate frame:

$$\alpha = T^{-1} \alpha^* T = \begin{bmatrix} 4.25 & 1.299 \\ 1.299 & 2.75 \end{bmatrix} \quad (21)$$

where:

$$T = \begin{bmatrix} \cos(30^\circ) & \sin(30^\circ) \\ -\sin(30^\circ) & \cos(30^\circ) \end{bmatrix} \quad (22)$$

Choosing K_e such that:

$$K_e = \begin{bmatrix} \frac{0.1}{s^2} & 0 \\ 0 & \frac{0.1}{s^2} \end{bmatrix} \text{ cm/Newton} \quad (23)$$

leads to left half-plane roots for $\det[I + GK_e E] = 0$. Due to limited space, the stability analysis has been omitted. Substituting G , E , α , and K_e from equations 13, 14, 17, 18, 21, and 23 into equation 8 results in an unrealizable transfer function matrix for K_h . In order to form K_h , reduced-order models were chosen to approximate members of $(G^{-1} E^{-1} + K_e)$ within a bounded frequency range. This choice of K_h results in low-pass transfer function for Δ_x and Δ_y . Members of K_h in the reduced form are then given by equation 24.

$$K_h = \begin{bmatrix} \frac{0.3}{s^2} \left(\frac{s^2}{31.31^2} + \frac{s}{89.17} + 1 \right) & 0 \\ 0 & \frac{0.31}{s^2} \left(\frac{s^2}{14.58^2} + \frac{s}{26.44} + 1 \right) \end{bmatrix} \alpha \quad (24)$$

Figure 6 depicts the table trajectory in an experiment where the human maneuvers the table irregularly (i.e., randomly). Irregular maneuvers create high and low frequency components in the table motion. Figures 7 and 8 show the measured forces f^*_e and f^*_h versus each other along both directions where force amplifications of 5 and 2 along x^* and y^* directions can be observed.

References

- 1) Clark, D.C. et al., "Exploratory Investigation of the Man-Amplifier Concept", U.S. Air Force AMRL-TDR-62-89, AD-390070, August 1962.
- 2) GE Company, "Exoskeleton Prototype Project, Final Report on Phase I", Report S-67-1011, Schenectady, NY, 66.
- 3) GE Company, "Hardiman I Prototype Project, Special Interim Study", Report S-68-1060, Schenectady, NY, 1968.
- 4) Groshaw, P. F., "Hardiman I Arm Test, Hardiman I Prototype", Report S-70-1019, GE Company, Schenectady, NY, 1969.
- 5) Kazerooni, H., "Human Machine Interaction via the Transfer of Power and Information Signals", IEEE Trans. on Systems, Man, and Cybernetics, Vol. 20, no 2, March 1990.
- 6) Kazerooni, H., "Loop Shaping Design Related to LQG/LTR for SISO Minimum Phase Plants", Int. Journal of Control, Volume 48, Number 1, July 1988.
- 7) Kazerooni, H., "On the Robot Compliant Motion Control," ASME J. of Dynamic Systems, and Control, Vol. 111, No. 3, September 1989.
- 8) Kazerooni, H., Sheridan, T. B., Houpt, P. K., "Robust Compliant Motion for Manipulators", IEEE J. of Robotics and Automation, Vo. 2, No. 2, June 1986.
- 9) Kazerooni, H., Waibel, B. J., and Kim, S., "Theory and Experiments on Robot Compliant Motion Control," ASME Journal of Dynamic Systems Measurements and Control, September 1990.
- 10) Kazerooni, H., "On the Contact Instability of the Robots When Constrained by Rigid Environments," IEEE Transactions on Automatic Control, Volume 35, Number 6, June 1990.
- 11) Lehtomaki, N.A., Sandell, N.R., Athans, M., "Robustness Results in Linear-Quadratic Gaussian Based Multivariable Control Designs", IEEE Trans. on Auto. Control, Vol. AC-26, No. 1, February 1981.
- 12) Makinson, B. J., "Research and Development Prototype for Machine Augmentation of Human Strength and Endurance, Hardiman I Project", Report S-71-1056, G. E. Company, NY, 1971.
- 13) Mizen, N. J., "Preliminary Design for the Shoulders and Arms of a Powered, Exoskeletal Structure", Cornell Aeronautical Lab. Rep. VO-1692-V-4, 1965.
- 14) Mosher, R.S., "Force Reflecting Electrohydraulic Servomanipulator", Electro-Technology, pp. 138, Dec. 60.
- 15) Mosher, R. S., " Handyman to Hardiman", SAE Report 670088.
- 16) Spong, M. W., Vidyasagar, M., "Robust Nonlinear Control of Robot Manipulator", IEEE Conference on Decision and Control, December 1985.

- 17) Stein, G., Athans, M., "The LQG/LTR Procedure for Multivariable Feedback Control Design", IEEE Trans. on Aut. Control, Vol. AC-32, No. 2, February 1987.

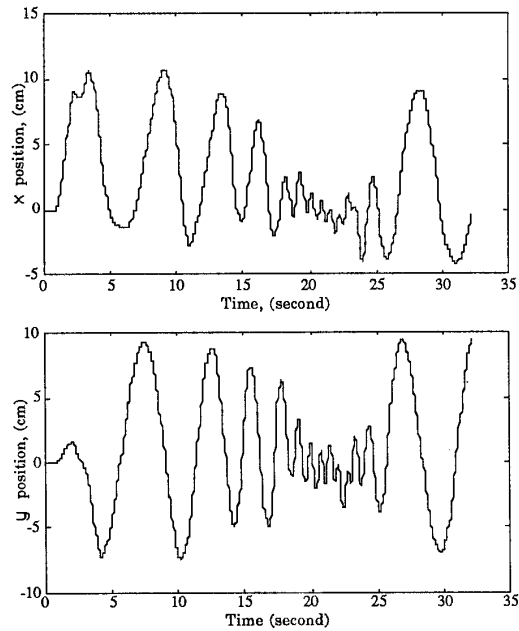


Figure 6: The Table Motion

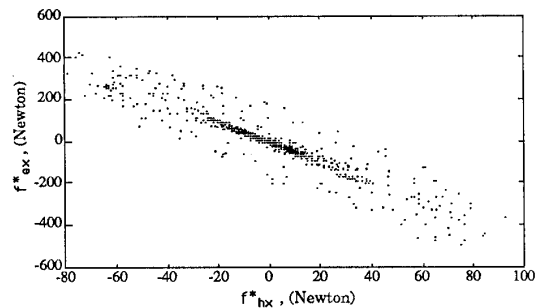


Figure 7: Force amplification by a factor of 5.

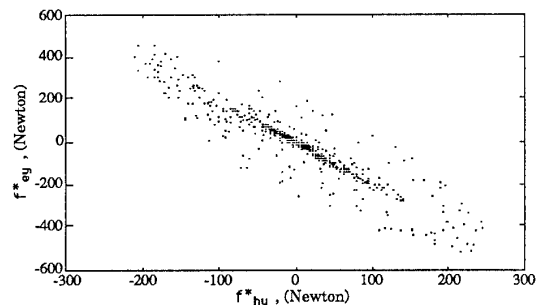


Figure 8: Force amplification by factor of 2.